Regulation of dendritic arborization by BCR Rac1 GTPase-activating protein, a substrate of PTPRT

A-Reum Park[1,2], Daeyoung Oh[3], So-Hee Lim[1], Jeonghoon Choi[2], Jeonghee Moon[1], Dae-Yeol Yu[4], Sung Goo Park[1], Nora Heisterkamp[5], Eunjoon Kim[3], Pyung-Keun Myung[5] and Jae-Ran Lee[1,*]

[1]Biomedical Proteomics Research Center, Korea Research Institute of Bioscience and Biotechnology, Daejeon 305-806, Korea
[2]College of Pharmacy, Chungnam National University, Daejeon 305-764, Korea
[3]Department of Biological Sciences, Korea Advanced Institute of Science and Technology, Daejeon 305-701, Korea
[4]Aging Research Center, Korea Research Institute of Bioscience and Biotechnology, Daejeon 305-806, Korea
[5]Section of Molecular Carcinogenesis, Division of Hematology/Oncology and The Saban Research Institute of Children's Hospital, Los Angeles, CA 90027, USA

*Author for correspondence (leejr@kribb.re.kr)

Accepted 7 June 2012
Journal of Cell Science 125, 4518–4531

doi: 10.1242/jcs.105502

Summary

Dendritic arborization is important for neuronal development as well as the formation of neural circuits. Rac1 is a member of the Rho GTPase family that serve as regulators of neuronal development. Breakpoint cluster region protein (BCR) is a Rac1 GTPase-activating protein that is abundantly expressed in the central nervous system. Here, we show that BCR plays a key role in neuronal development. Dendritic arborization and actin polymerization were attenuated by overexpression of BCR in hippocampal neurons. Knockdown of BCR using specific shRNAs increased the dendritic arborization as well as actin polymerization. The number of dendrites in null mutant $BCR^{-/-}$ mice was considerably increased compared with that in wild-type mice. We found that the function of the BCR GTPase-activating domain could be modulated by protein tyrosine phosphatase receptor T (PTPRT), which is expressed principally in the brain. We demonstrate that tyrosine 177 of BCR was the main target of PTPRT and the BCR mutant mimicking dephosphorylation of tyrosine 177 alleviated the attenuation of dendritic arborization. Additionally the attenuated dendritic arborization found upon BCR overexpression was relieved upon co-expression of PTPRT. When PTPRT was knocked down by a specific shRNA, the dendritic arborization was significantly reduced. The activity of the BCR GTPase-activating domain was modulated by means of conversions between the intra- and inter-molecular interactions, which are finely regulated through the dephosphorylation of a specific tyrosine residue by PTPRT. We thus show conclusively that BCR is a novel substrate of PTPRT and that BCR is involved in the regulation of neuronal development via control of the BCR GTPase-activating domain function by PTPRT.

Key words: Breakpoint cluster region, BCR, Protein tyrosine phosphatase receptor T, PTPRT, Fyn, Dendritic arborization, Actin polymerization

Introduction

Effective neural connections require appropriate navigations of axons to particular targets and the laborious construction of complex dendritic arbors to ensure the integration of synaptic signals. Dendrites must extend away from the originating neuronal soma into target fields to form connections with appropriate presynapses (Scott and Luo, 2001). The cytoskeletons of dendritic branches are composed of microtubules and cortical actin filaments lying close to the plasma membrane. During development the dendrites of neurons become branched and the extent of dendritic arborization correlates with the number of inputs (Van Aelst and Cline, 2004; Carlisle and Kennedy, 2005). The effects of neural activity on dendritic growth are known to be mediated by activation of small Rho GTPases (Chiu et al., 2008; Peng et al., 2009).

Rac1 is the most extensively studied member of the Rho GTPases that mediate morphological changes during neuronal development and serve as critical regulators of actin cytoskeletal formation (Chen and Firestein, 2009; Chen et al., 2010; Luo, 2000; Nakayama et al., 2000; Neubrand et al., 2010; Tahirovic et al., 2010). In response to extracellular signals, conversion between an inactive and an active form occurs via interaction with guanine nucleotide exchange factors (GEFs) and GTPase-activating proteins (GAPs) (Sfakianos et al., 2007; Bosco et al., 2009). Breakpoint cluster region protein (BCR), which is expressed abundantly in the brain, bears a Rac1 GAP domain in the C-terminal region (Chuang et al., 1995; Ress and Moelling, 2005; Rosso et al., 2005). Recently BCR has been shown to regulate synaptic plasticity as well as learning and memory in a process involving Rac1 GAP activity (Oh et al., 2010). However, the regulation mechanism of GAP activity is poorly understood.

Protein tyrosine phosphatase receptor T (PTPRT) is expressed principally in the central nervous system and regulates both neuronal synapse formation as well as synaptic transmission (Lim et al., 2009). Although a few substrates of PTPRT have been tentatively identified in cancer cells, no specific substrate for PTPRT during neuronal development has yet been discovered (Zhao et al., 2010). In the present work, mass spectrometry-based proteomics involving immunoprecipitation mediated by an antibody directed against PTPRT was applied to the rat synaptosome, and BCR was newly identified as a candidate neuronal substrate of PTPRT.

Here, we show that dendritic arborization and actin polymerization were attenuated by BCR overexpression in hippocampal neurons, but increased by knockdown of BCR

using shRNAs. Dendritic arborization was increased in null mutant ($BCR^{-/-}$) neurons. Tyrosine 177 located in the N-terminal region of BCR was dephosphorylated by PTPRT, and co-expression of PTPRT with BCR alleviated the attenuation of dendritic arborization. When PTPRT was knocked down in hippocampal neurons, dendritic arborization and polymerization of actin was decreased. The Rac1 GAP activity of BCR was controlled by means of a novel intramolecular interaction between the N- and C-termini of BCR; this activity was attenuated upon dephosphorylation by PTPRT. BCR thus serves as a new neuronal substrate of PTPRT and is a key regulator of neuronal development due to the BCR GAP activity controlled by PTPRT.

Results

BCR attenuates dendritic arborization and actin polymerization when serving as Rac1 GAPs

BCR and its close relative ABR (Active BCR Related or Actively transcribed BCR Related) are known to serve as GAPs for Rac1,

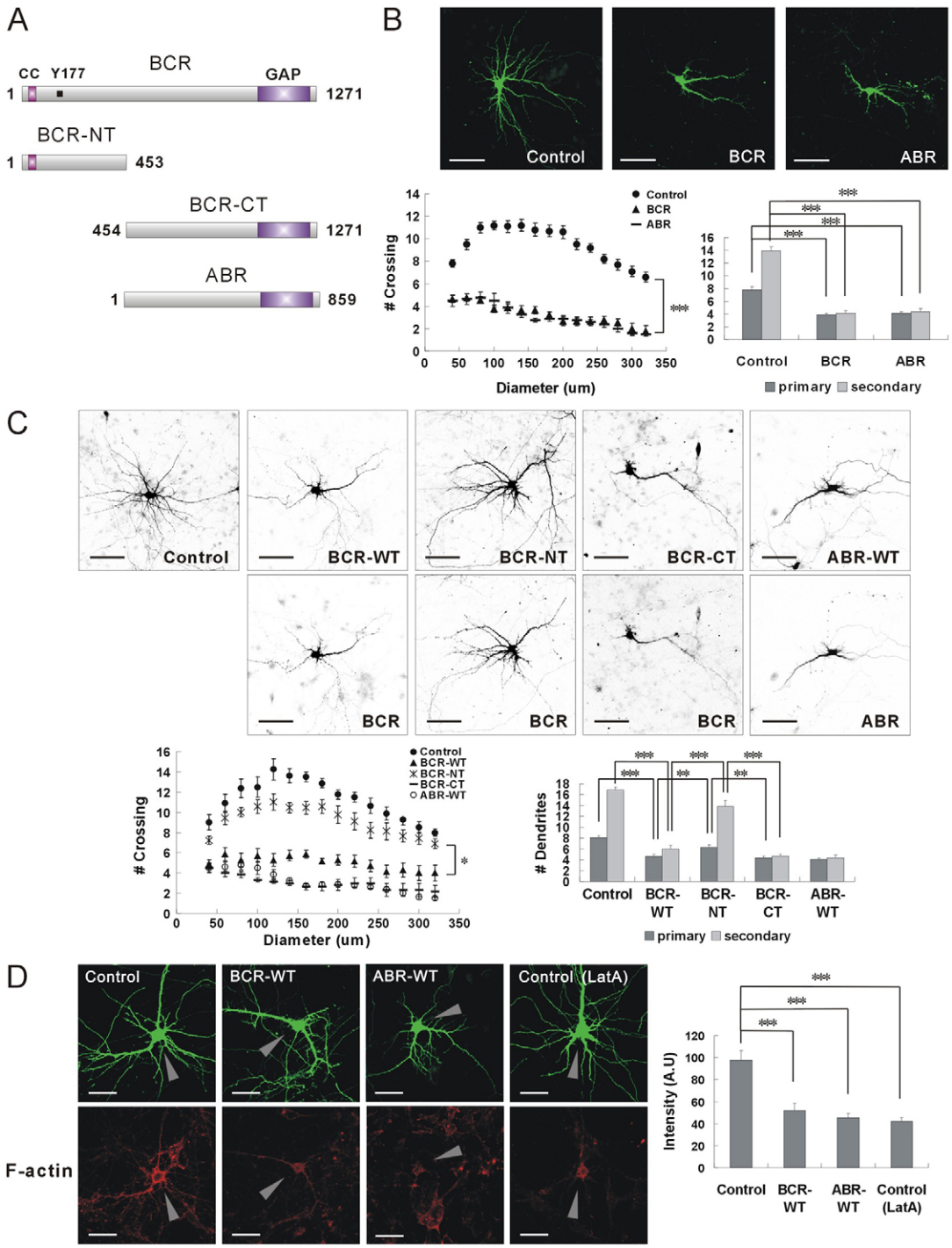

Fig. 1. See next page for legend.

Rac2, and Cdc42Hs, but to be inactive toward RhoA, Rap1A, and Ha-Ras (Chuang et al., 1995; Diekmann et al., 1991). BCR and ABR have a GAP domain within the C-terminal region but ABR has no functional domain in the N-terminus (Fig. 1A) (Heisterkamp et al., 1989; Tan et al., 1993). During rat brain development, the level of BCR expression was high at the embryonic stage and maintained slightly decreased levels throughout postnatal brain development, but the expression of ABR gradually increased (Oh et al., 2010). When BCR or ABR was overexpressed in cultured hippocampal neurons, the development of dendritic arborization was severely attenuated compared with control neurons that expressed EGFP only (Fig. 1B). Sholl profiles showed that overexpression of BCR or ABR significantly attenuated the dendritic arborization. The numbers of primary and secondary dendrites fell considerably upon overexpression of BCR or ABR. BCR has several enzymatically functional domains in the N-terminal region, but the GAP domain of the C-terminus appeared to be responsible for attenuation of arborization (Fig. 1C). When a BCR deletion mutant expressing the C-terminal region including the GAP domain (BCR-CT) was overexpressed, dendritic arborization was attenuated and the numbers of primary and secondary dendrites fell to levels comparable to those noted when wild-type BCR (BCR-WT) or ABR (ABR-WT) was overexpressed. However, a BCR deletion mutant expressing the N-terminal region (BCR-NT) had a phenotype similar to that of the control. Thus, dendritic arborization appeared to be controlled by BCR and ABR via a mechanism involving the Rac1 GAP domain.

Then level of F-actin was measured using phalloidin conjugated to a fluorophore to examine whether the Rac1 GAP activities of BCR and ABR changed the actin polymerization in cultured hippocampal neurons (Fig. 1D). Overexpression of BCR-WT or ABR-WT decreased actin polymerization of the neurons. The level of F-actin fell upon expression of BCR-WT or ABR-WT to the same degree as that of control neuron pretreated with Latrunculin A (Lat A), an inhibitor of actin polymerization. For normalized analysis, the F-actin intensities of background neurons that were grown on the same coverslips with neurons overexpressing BCR-WT, ABR-WT, or EGFP, were compared. The background neurons on each coverslip did not exhibit defferences in F-actin intensities, whereas the background F-actin intensity was significantly decreased after the Lat A-treatement (supplementary material Fig. S1A). Thus, BCR-WT and ABR-WT inhibited the actin polymerization of hippocampal neurons. Based on these data, dendritic arborization as well as actin polymerization appeared to be controlled by the Rac1 GAP activities of BCR and ABR.

Fig. 1. Dendritic arborization and actin polymerization are regulated by BCR and ABR Rac1 GAPs. (**A**) Schematic diagrams of BCR and ABR. BCR-NT and BCR-CT were constructed as described in the Materials and Methods. (**B**) The dendritic arborization of rat hippocampal neurons was attenuated upon overexpression of BCR and ABR Rac1 GAP. BCR and ABR, together with EGFP, or EGFP only (control) were overexpressed in cultured hippocampal neurons and their dendritic arborization was examined by staining with an anti-EGFP antibody. The extent of neuronal dendritic arborization was analyzed using Sholl profiling, and quantification of the numbers of primary and secondary dendrites. Overexpression of either BCR or ABR attenuated dendritic arborization. Means±s.e.m. for ten control neurons, nine BCR neurons and eight ABR neurons are shown. For primary dendrites: ***$P<0.001$, by the Newman-Keuls multiple comparison test after application of one-way ANOVA; $F=43.13$; $P<0.0001$. For secondary dendrites: ***$P<0.001$, by the Newman-Keuls multiple comparison test after application of one-way ANOVA; $F=135.4$; $P<0.0001$. Scale bar: 100 μm. (**C**) Attenuation of dendritic arborization by BCR GAP activity. Deletion mutants of BCR containing N- or C-half-termini (thus BCR-NT and BCR-CT) were overexpressed in hippocampal neurons. The dendritic arborization was attenuated by BCR-CT, which contains the GAP domain, to the same levels as those by BCR-WT or ABR-WT (WT, wild type). However, dendritic arborization was almost normal upon expression of BCR-NT. Expressions of BCR-WT, -NT, -CT and ABR-WT were examined by immunofluorescence with the aid of an anti-BCR or anti-ABR antibody, respectively. Means±s.e.m. were derived from eight control neurons, seven BCR-WT neurons, nine BCR-NT neurons, six BCR-CT neurons and eight ABR neurons. For primary dendrites: ***$P<0.001$ and **$P<0.01$, by the Newman-Keuls multiple comparison test after application of one-way ANOVA; $F=18.48$; $P<0.0001$. For secondary dendrites: ***$P<0.001$, by the Newman-Keuls multiple comparison test after application of one-way ANOVA; $F=51.64$; $P<0.0001$. Scale bar: 100 μm. (**D**) Actin polymerization was decreased when BCR-WT or ABR-WT was overexpressed in hippocampal neurons. The F-actin (polymerized actin) was stained with phalloidin conjugated with Alexa Fluor 555, and the level of actin polymerization was assessed in the neurons transfected with EGFP only (control), BCR-WT or ABR-WT together with EGFP (gray arrowhead). The average pixel intensities on all of the dendritic trunks per neuron were measured ~20 μm distant from the neuronal soma. Neurons overexpressing EGFP only were treated with Latrunculin A (Lat A), an inhibitor of actin polymerization and used as a negative control. The F-actin fluorescence intensity of BCR-WT or ABR-WT neurons was decreased to the same degree as that of control neurons pretreated with Lat A. The pixel intensities of the background neurons did not exhibit differences whereas that of the background neurons pretreated with Lat A was significantly decreased (supplementary material Fig. S1A). Means±s.e.m. of data from nine control neurons, nine BCR-WT neurons, eight ABR-WT neurons, and nine Lat A-treated control neurons are shown. ***$P<0.001$, by the Newman-Keuls multiple comparison test after application of one-way ANOVA; $F=19.88$; $P<0.0001$. Scale bar: 50 μm.

Dendritic arborization is increased by GAP activity inhibition or by BCR knockdown

Dendritic arborization appeared to be controlled by the Rac1 GAP activities of BCR and ABR. Therefore GAP-dead mutations, thus lacking GAP activities, were introduced into both BCR and ABR (Arg1,090 of BCR and Arg683 of ABR changed to Ala) and dendritic development was examined in these contexts (Fig. 2A,B) (Kawashima et al., 2000). Dendritic arborization was increased and the numbers of dendrites were significantly elevated compared with wild type when GAP-dead mutants of BCR or ABR (BCR-GD or ABR-GD) were applied. Moreover, the levels of actin polymerization were increased by GAP-dead mutants compared with wild type (supplementary material Fig. S2A,B). These results suggest that dendritic arborization could be controlled by BCR and ABR via a mechanism involving the Rac1 GAP activity.

To inhibit BCR expression in cultured hippocampal neurons, specific shRNAs were produced and expression of BCR was tested in the presence of BCR-shRNAs (Fig. 2C for BCR-shRNA; supplementary material Fig. S3B for BCR-shRNA*). Upon addition of BCR-shRNAs, expression of BCR was efficiently knocked down in rat hippocampal neurons (Fig. 2D; supplementary material Fig. S3A). When the effects of BCR knockdown on neuronal development were examined, dendritic arborization was significantly increased in BCR knockdown neurons compared with control neurons (sh-Vector) (Fig. 2E; supplementary material Fig. S3C). Then BCR constructs resistant to BCR-shRNAs (Resc BCR and Resc BCR*) (Fig. 2C; supplementary material Fig. S3B) were co-expressed in BCR knockdown neurons or were expressed

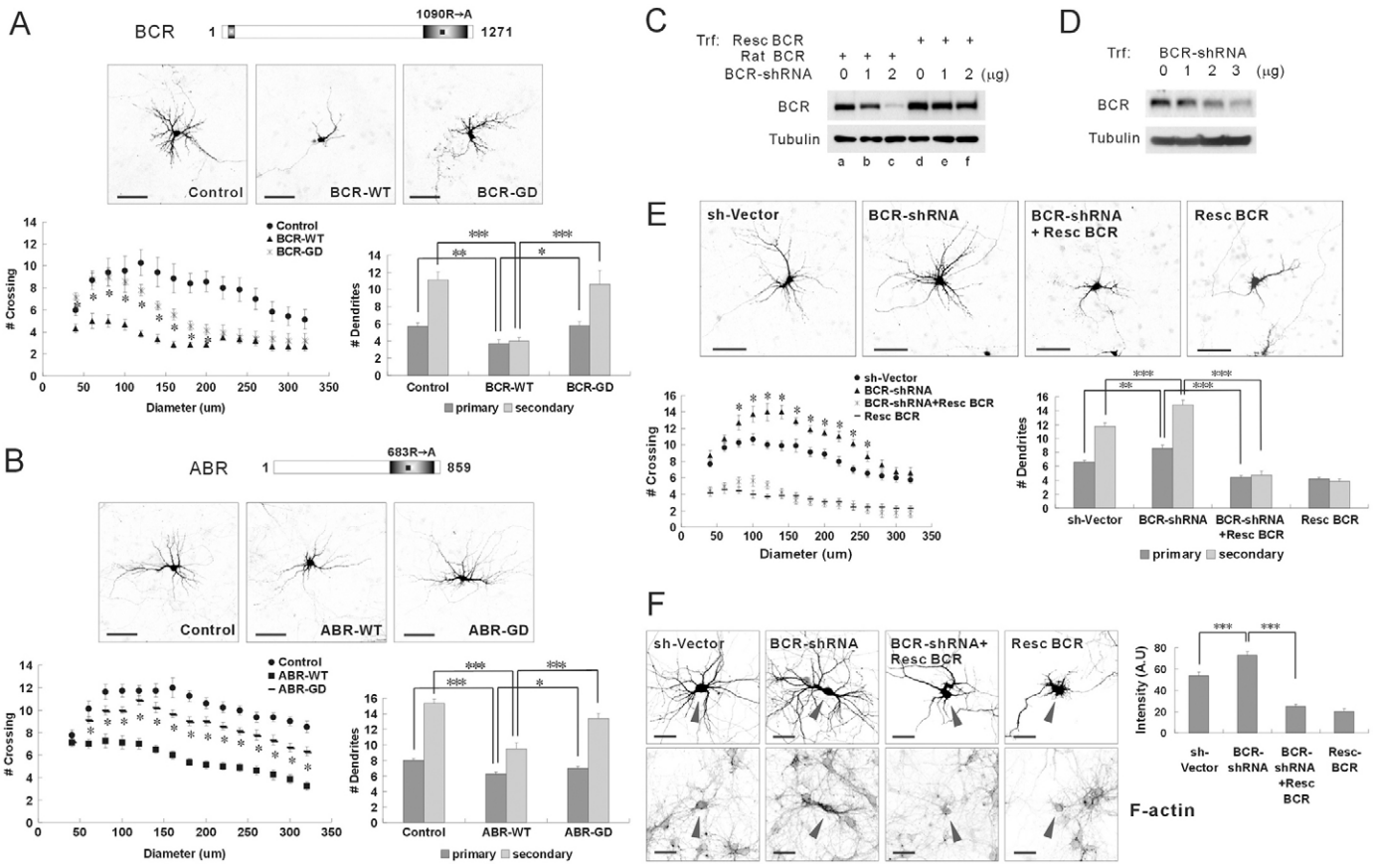

Fig. 2. Neuronal development is enhanced by Rac1 GAP activity inhibition and by BCR knockdown. (**A**) Rescue of dendritic arborization by a GAP-dead mutant of BCR (BCR-GD). The arborization was increased by a GAP-dead mutant of BCR (BCR-GD) compared with that of wild-type BCR (BCR-WT). Means±s.e.m. of data from seven control neurons, six BCR-WT neurons and five BCR-GD neurons are shown. For primary dendrites: $^{**}P<0.01$ and $^{*}P<0.05$, by the Newman-Keuls multiple comparison test after application of one-way ANOVA; $F=6.665$; $P=0.0085$. For secondary dendrites: $^{***}P<0.001$, by the Newman-Keuls multiple comparison test after application of one-way ANOVA; $F=15.66$; $P=0.0002$. Scale bar: 100 μm. (**B**) Rescue of arborization by a GAP-dead mutant of ABR. The arborization was increased by ABR-GD compared with ABR-WT. Means±s.e.m. of data from eight control neurons, eight ABR-WT neurons and nine ABR-GD neurons are shown. For primary dendrites: $^{***}P<0.001$ and $^{*}P<0.05$, by the Newman-Keuls multiple comparison test after application of one-way ANOVA; $F=11.80$; $P=0.0003$. For secondary dendrites: $^{***}P<0.001$, by the Newman-Keuls multiple comparison test after application of one-way ANOVA; $F=19.65$; $P<0.0001$. Scale bar: 100 μm. (**C**) BCR knockdown constructs were produced and the efficiencies were examined. Rat BCR and BCR-shRNA were co-expressed in HEK cells (a-c). The effect of shRNA was measured by immunoblotting the HEK cell lysate with an anti-BCR antibody. BCR was efficiently knocked down by BCR-shRNA. A BCR rescue construct with mutations of nucleotides in the shRNA target region (Resc BCR) was co-expressed with BCR-shRNA, and the expression level was measured by immunoblotting (d-f). The expression of Resc BCR was resistant to BCR-shRNA. Additional shRNA and rescue construct (BCR-shRNA* and Resc BCR*) were produced and their efficiencies were confirmed (supplementary material Fig. S3B). (**D**) The efficiency of BCR-shRNA was examined in rat cultured hippocampal neurons. When BCR-shRNA was transfected into neurons, a diminution of endogenous BCR was confirmed by western blotting (shown) and immunofluorescence (supplementary material Fig. S3A) with the aid of anti-BCR antibody. (**E**) Increased dendritic arborization upon knockdown of BCR. When rat hippocampal neurons were transfected with BCR-shRNA, the arborization was increased. However, the co-expression of Resc BCR with BCR-shRNA or single expression of Resc BCR decreased the number of dendrites to the level less than that of control neurons (expressing pSuper.gfp/neo vector: sh-Vector). This experiment generally gives less dendrites than those shown in Fig. 1 because of the younger hippocampal neurons used in the BCR knockdown experiments. Means±s.e.m. of data from seven control neurons, eight BCR-shRNA neurons, eight BCR-shRNA+Resc BCR neurons and seven Resc BCR neurons are shown. For primary dendrites: $^{**}P<0.01$ and $^{***}P<0.001$, by the Newman-Keuls multiple comparison test after application of one-way ANOVA; $F=13.93$; $P=0.0002$. For secondary dendrites: $^{***}P<0.001$, by the Newman-Keuls multiple comparison test after application of one-way ANOVA; $F=59.46$; $P<0.0001$. Scale bar: 100 μm. (**F**) Actin polymerization is enhanced by knockdown of BCR. The level of polymerized F-actin (gray arrowhead) was increased upon the knockdown of BCR and drop to a level less than that of control neurons upon co-expression of Resc BCR or single expression of Resc BCR. Means±s.e.m. of data from ten control neurons, twelve BCR-shRNA neurons, ten BCR-shRNA+Resc BCR neurons and nine Resc BCR neurons are shown. $^{***}P<0.001$ by the Newman-Keuls multiple comparison test after application of one-way ANOVA; $F=68.45$; $P<0.0001$. Scale bar: 50 μm.

without BCR-shRNAs. Expression of Resc BCR decreased dendritic arborization to the level less than control neurons.

Next, F-actin polymerization was examined in BCR knockdown neurons (Fig. 2F; supplementary material Fig. S3D). The level of F-actin was increased in BCR knockdown neurons compared with control neurons, but was reduced upon co-expression of Resc BCR or single expression of Resc BCR. The actin polymerization appeared to be enhanced when the Rac1 GAP activity was decreased by BCR knockdown, and to be attenuated by the rescued GAP activity when Resc BCR was co-expressed. Thus, dendritic arborization as well as actin polymerization was increased by BCR knockdown in hippocampal neurons.

Dendritic arborization is increased in BCR$^{-/-}$ mice neurons

The expression of BCR has been known to maintain slightly decreased levels throughout postnatal brain development compared with that of embryonic stage (Oh et al., 2010). We examined whether the developmental speed could be controlled through the deletion of the BCR genes. The expression of BCR in the brains was confirmed to decrease gradually from wild-type ($BCR^{+/+}$) to heterozygote ($BCR^{+/-}$) or null mutant ($BCR^{-/-}$) mice (Fig. 3A) (Voncken et al., 1995). When hippocampal neurons were prepared from $BCR^{+/-}$ or $BCR^{-/-}$, dendritic arborization and the numbers of primary and secondary dendrites increased gradually compared with $BCR^{+/+}$ neurons (Fig. 3B). This suggested that the development of hippocampal neurons could be regulated by a dosage of BCR expression. When BCR expression was rescued in $BCR^{-/-}$ neurons by overexpression of BCR-WT, the dendritic arborization of $BCR^{-/-}$ neurons was attenuated (Fig. 3C). Thus, BCR appeared to control the development of hippocampal neurons.

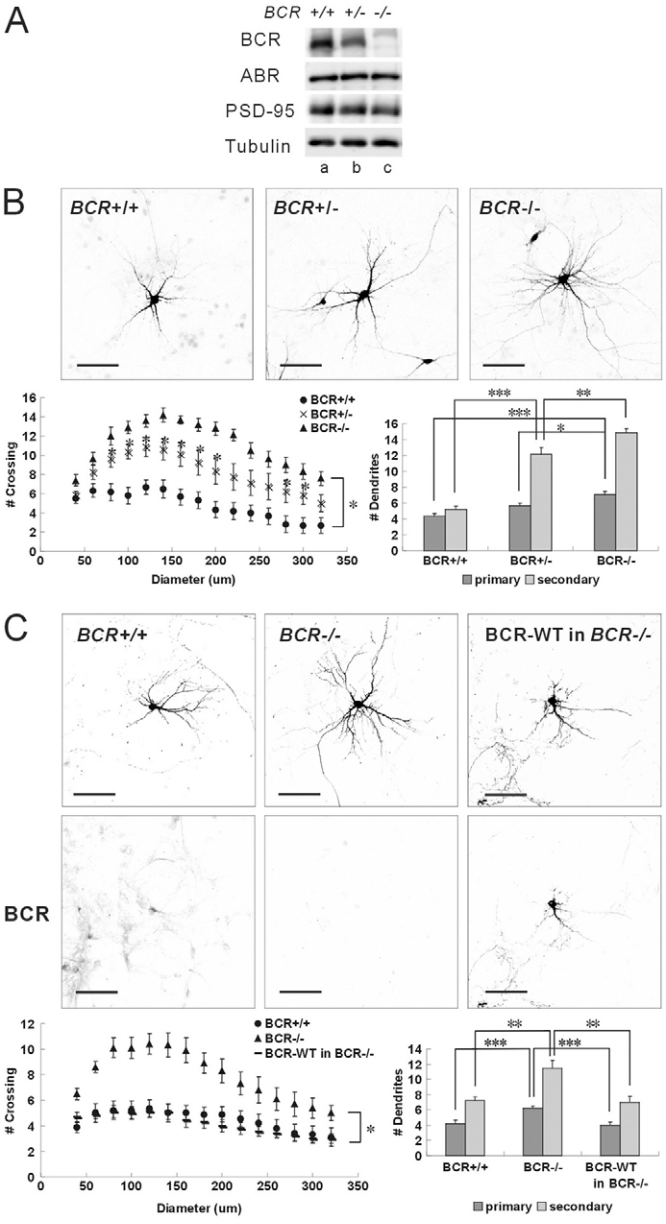

Dendritic arborization is increased by deletion of a coiled coil in the BCR N-terminus

The N-terminal coiled coil (CC) oligomerization domain of BCR has been known to be an important activator of the kinase activity of BCR-Abl oncogenes, and also supposed to promote the association of BCR-Abl with actin fibers (Pluk et al., 2002; Ren, 2005; Tauchi et al., 1997; Zhang et al., 2001). To determine whether the CC domain was involved in dendritic arborization, a BCR mutant lacking this region (BCR-ΔCC) was overexpressed in cultured hippocampal neurons (Fig. 4A). Both dendritic arborization and the numbers of primary and secondary dendrites were significantly increased by BCR-ΔCC compared with wild type. Deletion of the CC region appeared to inhibit the GAP activity of BCR, although the N-terminal CC is remote from the GAP domain of the C-terminus. If Rac1 GAP activity were decreased by deletion of the CC, differences in actin polymerization level should be evident upon expression of BCR-ΔCC. The actin polymerization was significantly increased by BCR-ΔCC compared with BCR-WT (Fig. 4B). Deletion of the CC in the N-terminus appeared to regulate the dendritic arborization as well as actin polymerization by controlling the BCR GAP activity.

In the case of overexpression in wild-type neurons, the phenotype could be originated from the dominant-negative effects. Therefore, all BCR constructs were expressed in $BCR^{-/-}$ mice neurons and the phenotypes were compared with those of wild-type neurons (Fig. 4C). When BCR-WT was overexpressed in $BCR^{-/-}$ neurons, dendritic arborization was severely attenuated similar to that in wild-type neurons. The dendritic arborization was increased by BCR-ΔCC in $BCR^{-/-}$ neurons similar to wild-type neurons. BCR-CT-deletion mutants

Fig. 3. Dendritic arborization is increased in BCR null mutant mice. (**A**) Expression of BCR was examined in a brain of wild-type, $BCR^{+/-}$ and $BCR^{-/-}$ null mutant mice by immunoblotting with an anti-BCR antibody. BCR expression was significantly lower in the brain of a heterozygote compared with that in a wild-type mouse, and was completely absent in the brain of a homozygote animal. (**B**) Increased dendritic arborization in hippocampal neurons of $BCR^{+/-}$ and $BCR^{-/-}$ mice. Cultured neurons were prepared from hippocampi of wild-type, heterozygote or homozygote mice, and EGFP was overexpressed for examination of dendritic arborization. The dendritic arborization of $BCR^{+/-}$ and $BCR^{-/-}$ neurons was increased compared to the level seen in wild-type mice. The number of dendrites in mice neurons was generally less than that in rat neurons. Means±s.e.m. of data from six wild-type neurons, eight $BCR^{+/-}$ neurons and ten $BCR^{-/-}$ neurons are shown. For primary dendrites: $^{***}P<0.001$ and $^{*}P<0.05$, by the Newman-Keuls multiple comparison test after application of one-way ANOVA; $F=9.859$; $P=0.001$. For secondary dendrites: $^{***}P<0.001$ and $^{**}P<0.01$, by the Newman-Keuls multiple comparison test after application of one-way ANOVA; $F=50.53$; $P<0.0001$. Scale bar: 100 μm. (**C**) Overexpression of BCR-WT decreased dendritic arborization in hippocampal neurons of $BCR^{-/-}$ mice. The dendritic arborization of $BCR^{-/-}$ neurons fell to the level noted in wild-type neurons upon transfection with BCR-WT. BCR expression was examined by immunofluorescence with the aid of an anti-BCR antibody. Means±s.e.m. of data from nine wild-type neurons, eleven $BCR^{-/-}$ neurons and nine BCR-WT in $BCR^{-/-}$ neurons are shown. For primary dendrites: $^{***}P<0.001$, by the Newman-Keuls multiple comparison test after application of one-way ANOVA; $F=12.19$; $P=0.0002$. For secondary dendrites: $^{**}P<0.01$, by the Newman-Keuls multiple comparison test after application of one-way ANOVA; $F=9.098$; $P=0.001$. Scale bar: 100 μm.

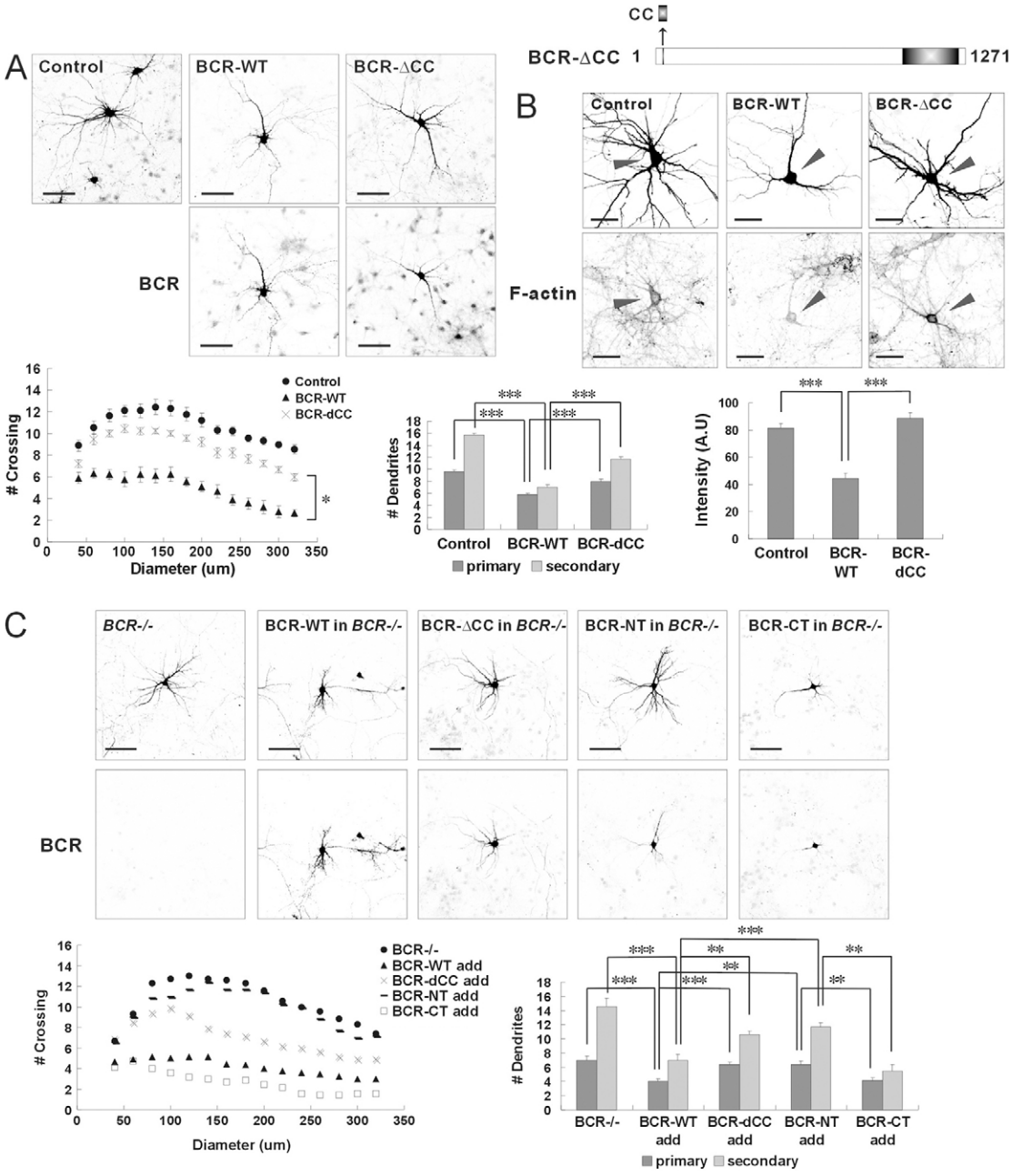

Fig. 4. Dendritic arborization is increased by deletion of the BCR N-terminal coiled coil. (**A**) Increased arborization of rat neurons upon deletion of the coiled-coil region in the N-terminus of BCR. The N-terminal coiled-coil domain was deleted from BCR to yield the BCR-ΔCC mutant, resulting in markedly increased dendritic arborization. Means±s.e.m. of data from ten control neurons, nine BCR-WT neurons, and nine BCR-ΔCC neurons are shown. For primary dendrites: ***$P<0.001$, by the Newman-Keuls multiple comparison test after application of one-way ANOVA; $F=34.20$; $P<0.0001$. For secondary dendrites: ***$P<0.001$, by the Newman-Keuls multiple comparison test after application of one-way ANOVA; $F=97.13$; $P<0.0001$. Scale bar: 100 µm. (**B**) Actin polymerization was increased by deletion of the BCR coiled coil. The level of F-actin (gray arrowhead) was increased when BCR-ΔCC was overexpressed compared with that of BCR-WT. Means±s.e.m. of data from ten control neurons, eight BCR-WT neurons and seven BCR-ΔCC neurons are shown. ***$P<0.001$, by the Newman-Keuls multiple comparison test after application of one-way ANOVA; $F=15.37$; $P<0.0001$. Scale bar: 50 µm. (**C**) Overexpression of BCR constructs gave the same phenotypes in $BCR^{-/-}$ mice neurons as seen in wild-type neurons. The dendritic arborization was attenuated by overexpression of BCR-WT and increased by BCR-ΔCC in $BCR^{-/-}$ neurons. BCR-CT constructs attenuated arborization of $BCR^{-/-}$ neurons whereas BCR-NT did not. Means±s.e.m. of data from seven $BCR^{-/-}$ neurons, nine BCR-WT neurons, eight BCR-ΔCC neurons, seven BCR-NT neurons and seven BCR-CT neurons are shown. For primary dendrites: ***$P<0.001$ and **$P<0.01$, by the Newman-Keuls multiple comparison test after application of one-way ANOVA; $F=10.84$; $P<0.0001$. For secondary dendrites: ***$P<0.001$ and **$P<0.01$, by the Newman-Keuls multiple comparison test after application of one-way ANOVA; $F=19.07$; $P<0.0001$. Scale bar: 100 µm.

containing a GAP domain decreased dendrites of $BCR^{-/-}$ whereas BCR-NT did not induce any change of phenotype in $BCR^{-/-}$ neurons. These data suggest that the changes of phenotype were not from the dominant-negative effects, but BCR constructs changed the dendritic arborization with Rac1 GAP activity.

BCR is a new neuronal substrate of PTPRT

BCR was newly identified as a possible interaction partner of PTPRT through mass spectrometry-based proteomics that were used to analyze immunoprecipitated rat brain synaptosome proteins employing an anti-PTPRT-specific monoclonal antibody (Fig. 5A,B). Using the Mascot database search program, the amino acid sequences of the combined MS/MS spectra of peptide ions were identified as those of BCR. BCR was efficiently pulled down by PTPRT in deoxycholate-extracted rat synaptosomes (Fig. 5C). Although BCR has no functional trans-membrane domains, it was localized to the membrane fractions of the rat brain (Oh et al., 2010). Therefore, BCR appeared to interact with the receptor-type phosphatase PTPRT that was primarily localized to the membrane fractions (Lim et al., 2009). When the BCR and PTPRT constructs were co-expressed in HEK cells, BCR interacted principally with the catalytic domain of PTPRT (the RT-JD domain), whereas the full-length PTPRT (exemplified by RT-FL) showed weak interactions with BCR (Fig. 5D,E; supplementary material Fig. S4). In HEK cells, overexpressed BCR was localized primarily in the cytosol, and the full-length PTPRT was localized to the membrane fractions. In contrast, the RT-JD, a deletion mutant of PTPRT was primarily localized in the cytosol through deletion of

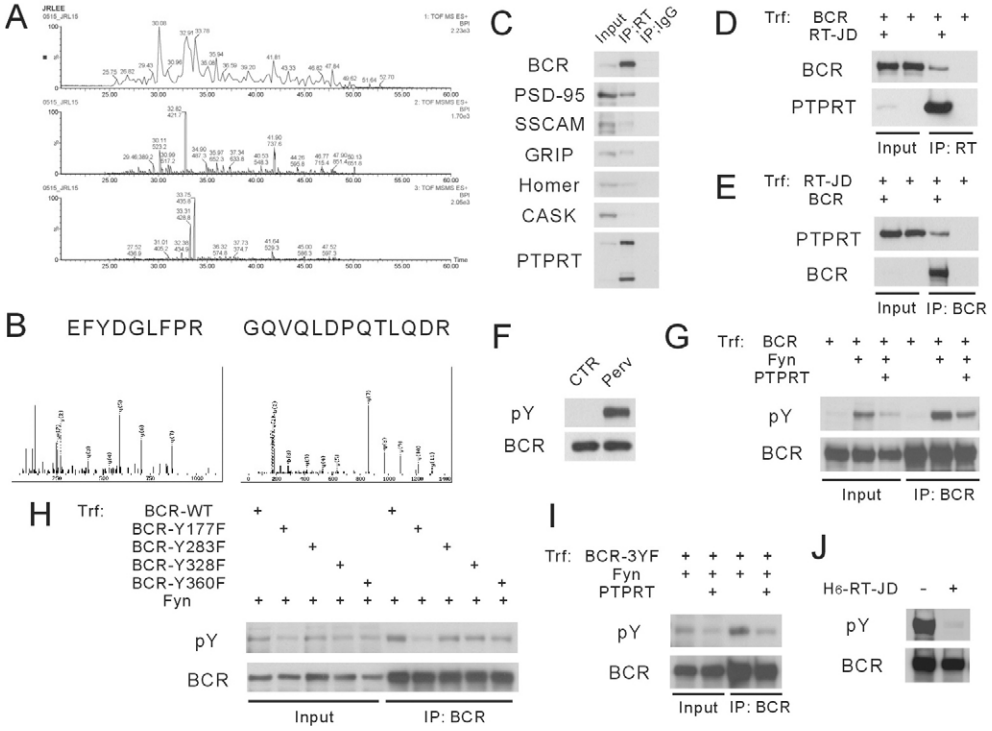

Fig. 5. BCR is a novel substrate of PTPRT. (**A**) Representative base peak chromatograms of mass spectrometry generated in MS and MS/MS modes. The top panel shows the base peak chromatogram of the MS survey scan, and the lower two panels are the base peak chromatograms from the MS/MS channels. (**B**) Combined MS/MS spectra of BCR peptide ions. The amino acid sequences were identified using the Mascot database search program. The matched fragment ion peaks for the most probable sequence are labeled on the spectra. (**C**) Co-immunoprecipitation of rat brain synaptosome proteins. BCR was co-precipitated by an anti-PTPRT monoclonal antibody. Input: 10%. Quantification (immunoprecipitated, IP/input proteins): BCR, 3.5; PSD-95, 0.46; SSCAM, 0.43; GRIP, 0.60; Homer, 0.64; CASK, 0.28; PTPRT, 5.59. (**D**,**E**) Co-immunoprecipitation was conducted using BCR and deletion mutant of PTPRT in HEK cells. BCR and PTPRT interact via an intracellular catalytic domain. BCR was pulled down by the catalytic domain of PTPRT (RT-JD), and RT-JD was pulled down by BCR, respectively. Quantification (immunoprecipitated, IP/input proteins): (D) BCR pulled down by RT-JD, 0.24; (E) RT-JD pulled down by BCR, 0.40. (**F**) Phosphorylation of BCR tyrosine residues in cultured hippocampal neurons. After hippocampal neurons were solubilized, endogenous BCR was immunoprecipitated. When cultured neurons were treated with pervanadate, a potent inhibitor of tyrosine phosphatases, the tyrosine residue of BCR was phosphorylated. CTR, control; Perv, pervanadate-treated; pY, phosphorylated tyrosine. (**G**) BCR is phosphorylated by Fyn and dephosphorylated by PTPRT. The level of the phosphorylated BCR increased when the Fyn was co-expressed with BCR, and fell upon expression of PTPRT, in HEK cells. Quantification (dephosphorylated/phosphorylated BCR): BCR-WT, 0.67. pY, phosphorylated tyrosine. (**H**) Tyrosine 177 of BCR is a major target of Fyn. The level of the phosphorylated BCR was decreased by mutation of tyrosine 177 to phenylalanine by more than when tyrosine residues 283, 328 or 360 were mutated. Quantification (mutated/wild-type BCR): BCR-Y177F, 0.33; BCR-Y283F, 0.87; BCR-Y328F, 0.76; BCR-Y360F, 0.76. pY, phosphorylated tyrosine. (**I**) Tyrosine 177 is a major target of PTPRT. The level of the phosphorylated BCR triple-mutant protein mimicking non-phosphorylation of tyrosine residues 283, 328 and 360 (by mutation to phenylalanine), thus with tyrosine 177 intact (BCR-3YF), was markedly reduced by PTPRT compared with that of BCR-WT. Quantification (dephosphorylated/phosphorylated BCR): BCR-3YF, 0.32 (compare with BCR-WT, 0.67 in Fig. 5G). pY, phosphorylated tyrosine. (**J**) Recombinant PTPRT dephosphorylates BCR. Purified recombinant proteins carrying the PTPRT catalytic domain (H_6-RT-JD) were added to the BCR proteins that were expressed in HEK cells and then precipitated by anti-BCR antibody following treatment with pervanadate. Tyrosine residues of BCR were significantly dephosphorylated by the recombinant PTPRT catalytic domain. pY, phosphorylated tyrosine.

the trans-membrane domain. As a result, BCR appeared to interact strongly with the RT-JD, but not with full-length PTPRT.

Tyrosine residues of BCR were phosphorylated in hippocampal neurons treated with pervanadate, a potent inhibitor of protein tyrosine phosphatase (Fig. 5F). Previously, the neuronal tyrosine kinase Fyn was shown to interact with PTPRT and to regulate the activity of PTPRT (Lim et al., 2009). In the present work, Fyn was shown to phosphorylate BCR and expression of PTPRT decreased the phosphorylation of BCR (Fig. 5G). BCR may thus be a neuronal substrate of the Fyn tyrosine kinase and the PTPRT tyrosine phosphatase. In myeloid cells, BCR is known to be phosphorylated on tyrosine residues within the first exon; the relevant residues are tyrosines 177, 283, and 360 (Li and Smithgall, 1996; Liu et al., 1996; Sini et al., 2004). BCR mutants mimicking tyrosine non-phosphorylation were created, and phosphorylation levels were examined to identify the main target of Fyn (Fig. 5H). A BCR mutant mimicking non-phosphorylation of tyrosine 177 showed significantly reduced tyrosine phosphorylation; tyrosine

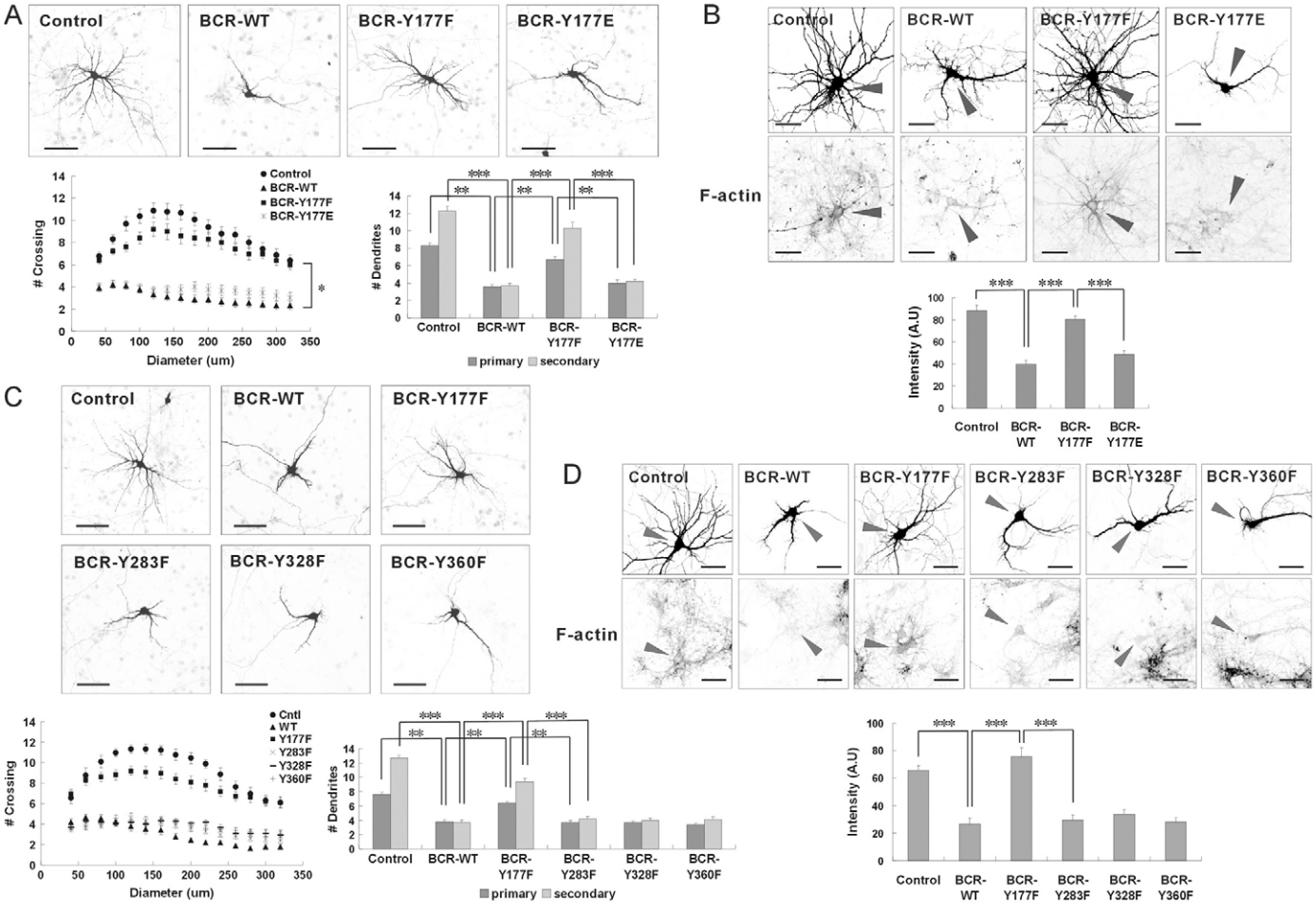

Fig. 6. A BCR mutant mimicking dephosphorylation of tyrosine 177 increases dendritic arborization. (**A**) The dendritic arborization is increased by a BCR mutant mimicking dephosphorylation in rat hippocampal neurons. BCR-Y177F rescued the dendritic arborization. When a BCR-Y177E was employed, the extent of arborization was similar to that seen in the presence of BCR-WT. Means±s.e.m. of data from nine control neurons, eight BCR-WT neurons, seven BCR-Y177F neurons and six BCR-Y177E neurons are shown. For primary dendrites: $^{**}P<0.01$, by the Newman-Keuls multiple comparison test after application of one-way ANOVA; $F=13.75$; $P<0.0001$. For secondary dendrites: $^{***}P<0.001$, by the Newman-Keuls multiple comparison test after application of one-way ANOVA; $F=105.2$; $P<0.0001$. Scale bar: 100 µm. (**B**) Actin polymerization is increased by expression of BCR-Y177F. The level of polymerized F-actin (gray arrowhead) increased when BCR-Y177F was overexpressed compared with that of BCR-WT. BCR-Y177E did not enhance F-actin polymerization compared with BCR-WT. Means±s.e.m. of data from six control neurons, eight BCR-WT neurons, seven BCR-Y177F neurons and seven BCR-Y177E neurons are shown. $^{***}P<0.001$, by the Newman-Keuls multiple comparison test after application of one-way ANOVA; $F=19.10$; $P<0.0001$. Scale bar: 50 µm. (**C**) BCR carrying mutations in tyrosine residues other than tyrosine 177 did not rescue dendritic arborization. When the BCR tyrosine residues 283, 328 and 360 were changed to phenylalanine (BCR-Y283F, -Y328F and -Y360F), the dendritic arborization was not increased, in contrast to what was observed when tyrosine 177 was mutated. Means±s.e.m. of data from eight control neurons, seven BCR-WT neurons, six BCR-Y177F neurons, seven BCR-Y283F neurons, seven BCR-Y328F neurons and nine BCR-Y360F neurons are shown. For primary dendrites: $^{**}P<0.01$, by the Newman-Keuls multiple comparison test after application of one-way ANOVA; $F=11.49$; $P<0.0001$. For secondary dendrites: $^{***}P<0.001$, by the Newman-Keuls multiple comparison test after application of one-way ANOVA; $F=82.85$; $P<0.0001$. Scale bar: 100 µm. (**D**) BCR proteins carrying mutations in tyrosine residues other than tyrosine 177 did not increase actin polymerization. BCR-Y283F, -Y328F, and -Y360F did not increase the level of polymerized F-actin (gray arrowhead) compared with that of BCR-WT. Means±s.e.m. of data from twelve control neurons, twelve BCR-WT neurons, eleven BCR-Y177F neurons, twelve BCR-Y283F neurons and twelve BCR-Y177E neurons are shown. $^{***}P<0.001$, by the Newman-Keuls multiple comparison test after application of one-way ANOVA; $F=11.59$; $P<0.0001$. Scale bar: 50 µm.

177 was thus shown to be the principal target of the Fyn tyrosine kinase. To determine whether tyrosine 177 was also the main target of PTPRT, a BCR triple mutant mimicking non-phosphorylation of all of tyrosines 283, 328, and 360, thus excluding tyrosine 177 (BCR-3YF), was created, and the level of tyrosine phosphorylation were examined (Fig. 5I). The level of phosphorylation was markedly reduced by expression of PTPRT, and tyrosine 177 was thus shown to be the main target of PTPRT. To confirm that BCR was a novel substrate of PTPRT, purified recombinant proteins containing the PTPRT catalytic domain were admixed with recombinant BCR protein precipitated by anti-BCR antibody from cell lysates (fluids containing the contents of lysed cell) after treatment with pervanadate (Fig. 5J). The catalytic domain of PTPRT significantly reduced BCR phosphorylation, and thus BCR was unequivocally identified as a novel substrate of PTPRT in hippocampal neurons.

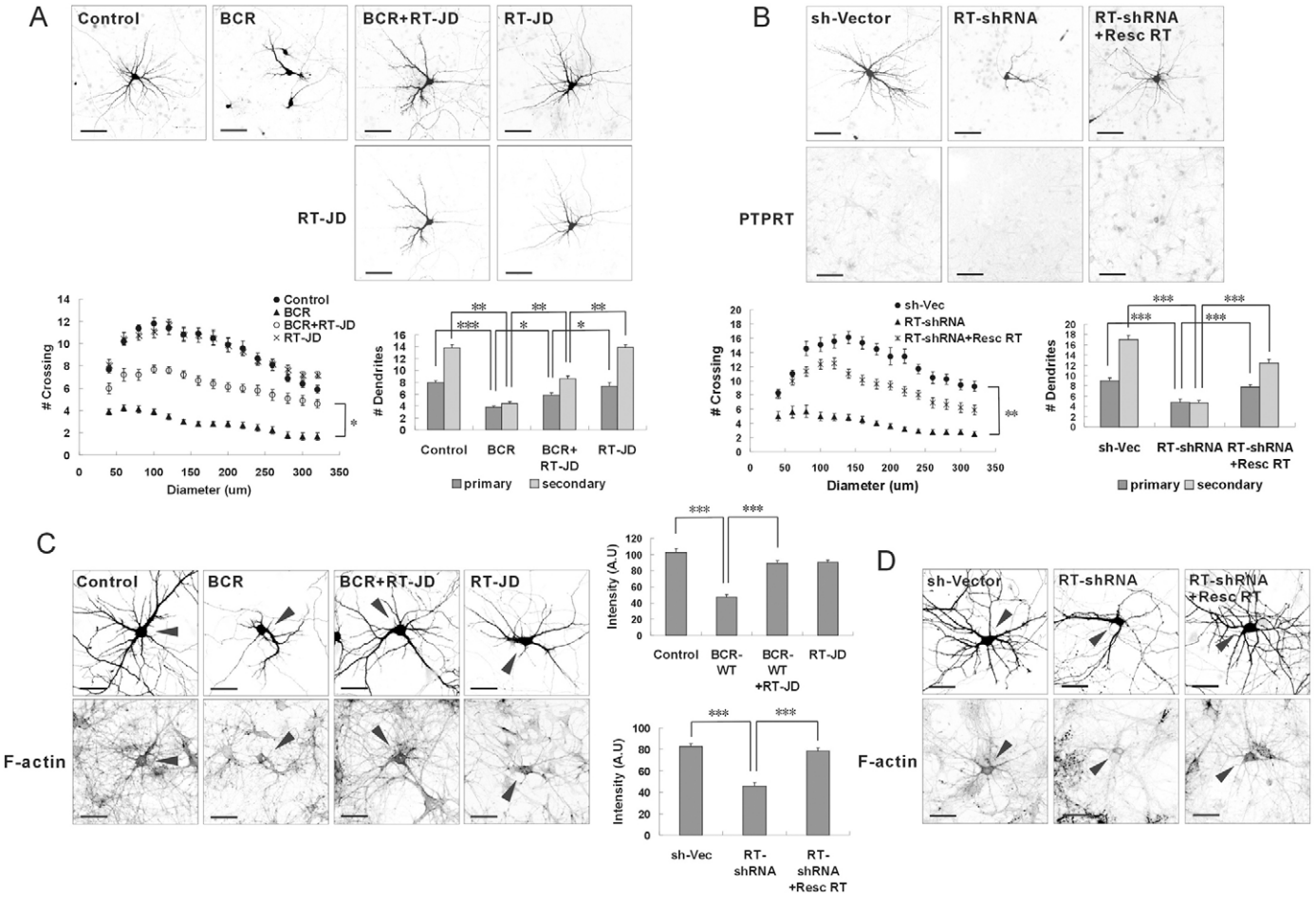

Fig. 7. Dendritic arborization and actin polymerization are rescued by PTPRT. (**A**) Dendritic arborization is rescued by PTPRT. The co-expression of the PTPRT catalytic domain (RT-JD) rescued the dendritic arborization that was attenuated by BCR in rat hippocampal neurons. When only RT-JD was expressed, the number of dendrites was not changed compared with control. Expression of RT-JD was visualized by immunofluorescence using an anti-PTPRT antibody. Means±s.e.m. of data from ten control neurons, nine BCR neurons, ten BCR+RT-JD neurons and nine RT-JD neurons are shown. For primary dendrites: ***$P<0.001$ and *$P<0.05$, by the Newman-Keuls multiple comparison test after application of one-way ANOVA; $F=20.26$; $P<0.0001$. For secondary dendrites: **$P<0.01$, by the Newman-Keuls multiple comparison test after application of one-way ANOVA; $F=124.0$; $P<0.0001$. Scale bar: 100 μm. (**B**) Attenuated dendritic arborization upon knockdown of PTPRT. When rat hippocampal neurons were transfected with PTRPT-shRNA (Lim et al., 2009), the numbers of dendrites and arborization were significantly decreased and rescued by the addition of Resc PTPRT to this context. Means±s.e.m. of data from nine control neurons, ten PTPRT-shRNA neurons, and nine PTPRT-shRNA+Resc PTPRT neurons are shown. For primary dendrites: ***$P<0.001$, by the Newman-Keuls multiple comparison test after application of one-way ANOVA; $F=16.66$; $P<0.0001$. For secondary dendrites: ***$P<0.001$, by the Newman-Keuls multiple comparison test after application of one-way ANOVA; $F=85.29$; $P<0.0001$. Scale bar: 100 μm. (**C**) Actin polymerization is rescued by RT-JD. The level of F-actin (gray arrowhead) increased upon co-expression of the RT-JD. When RT-JD was singly expressed, the level of actin polymerization was not different from that of control. Means±s.e.m. of data from nine control neurons, ten BCR neurons, ten BCR+RT-JD neurons and ten RT-JD neurons are shown. ***$P<0.001$, by the Newman-Keuls multiple comparison test after application of one-way ANOVA; $F=45.97$; $P<0.0001$. Scale bar: 50 μm. (**D**) Knockdown of PTPRT attenuated actin polymerization. When the expression of PTPRT was knocked down using PTPRT-shRNA, the level of F-actin (gray arrowhead) significantly decreased compared with control and was rescued by the addition of Resc PTPRT. Means±s.e.m. of data from nine control neurons, ten PTPRT-shRNA neurons and ten PTPRT-shRNA+Resc PTPRT neurons are shown. ***$P<0.001$ by the Newman-Keuls multiple comparison test after application of one-way ANOVA; $F=46.10$; $P<0.0001$. Scale bar, 50 μm.

The Rac1 GTPase pathway is regulated by dephosphorylation of BCR

Then, the effect of the tyrosine dephosphorylation of BCR on the dendritic arborization was explored. When a mutant mimicking dephosphorylation of tyrosine 177 (BCR-Y177F) was overexpressed, neuronal development was significantly increased compared with that of BCR-WT (Fig. 6A). When a mutant mimicking phosphorylation (thus with tyrosine mutated to glutamate; BCR-Y177E) was overexpressed in the neuron, the dendritic arborization was attenuated and the numbers of dendrites fell to levels comparable to those of wild-type BCR. The BCR-Y177F and -Y177E proteins were confirmed to be expressed at similar levels in hippocampal neurons (data not shown). BCR-Y177F significantly increased the actin polymerization compared with BCR-WT, whereas BCR-Y177E did not (Fig. 6B). BCR mutants mimicking dephosphorylation of other tyrosine residues, the BCR-Y283F, -Y328F, and -Y360F mutants, failed to increase either dendritic arborization or actin polymerization (Fig. 6C,D). Therefore, we suggest that dephosphorylation of tyrosine 177 inhibits the GAP activity of BCR, and consequently activates a Rac1 GTPase pathway effective to increase both actin polymerization and neuronal development.

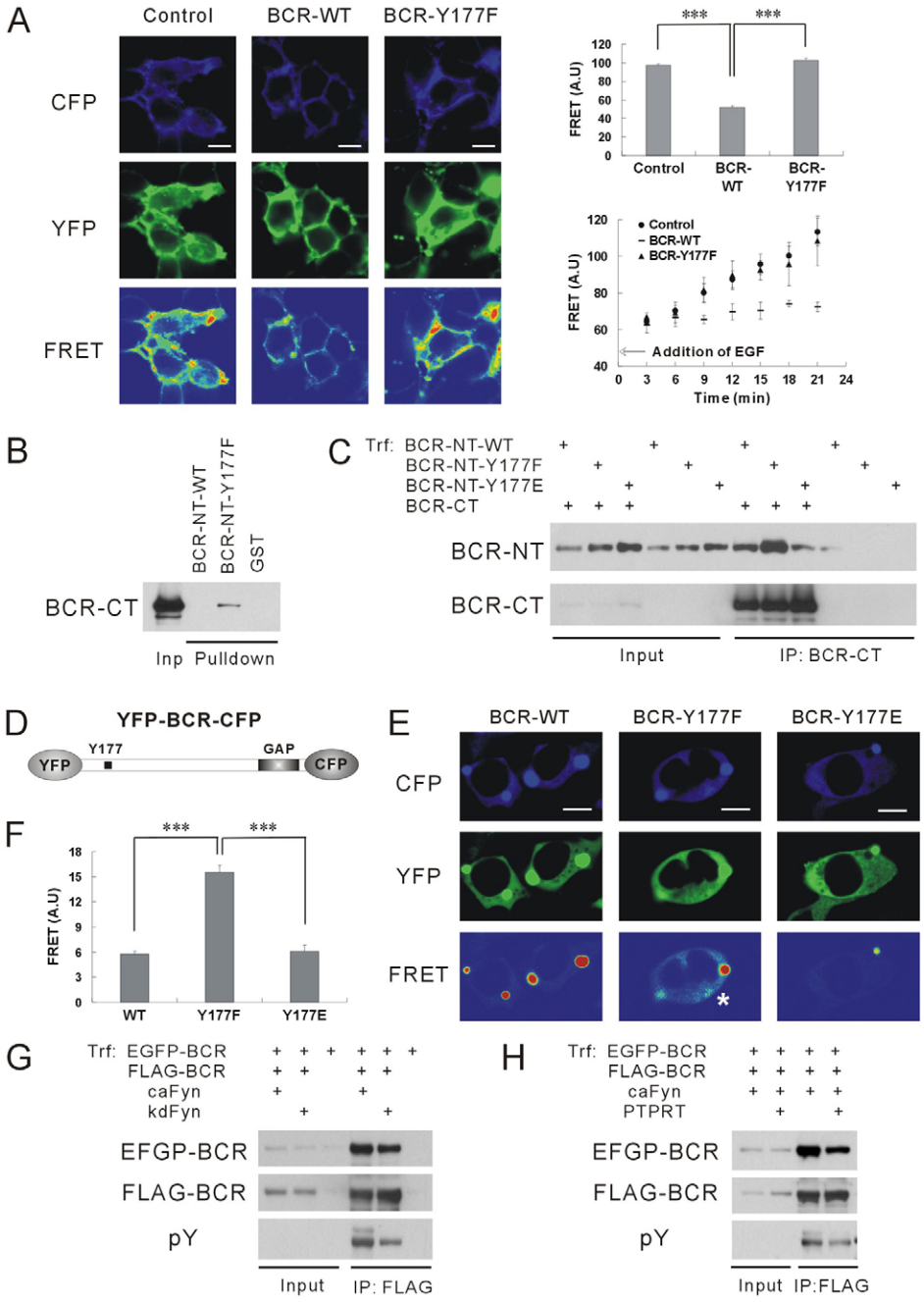

Fig. 8. See next page for legend.

Dendritic arborization is regulated by PTPRT

PTPRT has been known to regulate neuronal synapse formation through its catalytic activity (Lim, 2009). In this present work, possible roles of PTPRT in the neuronal development, mediated by interaction with BCR Rac1 GAP, were explored in detail. When PTPRT catalytic domains (RT-JD) were co-expressed with BCR, the attenuation of dendritic arborization was significantly relieved (Fig. 7A). Although full-length PTPRT seemed relatively ineffective in this respect (data not shown), expression of RT-JD rescued the neuronal development attenuated upon BCR overexpression. Single expression of RT-JD or full-length PTPRT did not affect the arborization. However, the knockdown of PTPRT attenuated the development of hippocampal neurons (Fig. 7B). Previously, PTPRT expression was efficiently knocked down using a specific PTPRT-shRNA and was rescued by addition of PTPRT construct resistant to PTPRT-shRNA (Resc PTPRT) in rat cultured neurons (Lim et al., 2009). In this work, the dendritic arborization was dramatically decreased through the application of PTPRT-shRNA and rescued by addition of Resc PTPRT.

Actin polymerization was significantly rescued by co-expression of RT-JD with BCR, whereas single expression of RT-JD showed no more actin polymerization compared with control neurons (Fig. 7C; supplementary material Fig. S1G). When PTPRT was knocked down, the actin polymerization was significantly decreased and rescued by co-expression of Resc PTPRT (Fig. 7D; supplementary material Fig. S1H). From these data, PTPRT was able to regulate the development through its catalytic activity, rescuing both dendritic arborization and actin polymerization attenuated by overexpression of BCR.

Rac1 GAP activity of BCR is regulated by PTPRT

In the next step, the Rac1 GAP activity of BCR was measured in living cells using a Rac1-FRET (Fluorescence Resonance Energy Transfer) sensor, which induces a FRET signal when Rac1 GTPase is activated (Fig. 8A). When BCR-WT was co-expressed with the Rac1-FRET sensor in COS 7 cells, the intensities of FRET signal were significantly reduced compared to the single expression of the Rac1-FRET sensor (control). On the other hand, the co-expression of BCR-Y177F, a mutant mimicking dephosphorylation, increased the intensity of the FRET signal similar to the control. These results show that BCR can inactivate Rac1GTPase through its GAP activity and that the GAP activity of BCR could be controlled through dephosphorylation of tyrosine 177 by PTPRT.

How could PTPRT control C-terminal GAP activity via dephosphorylation of a tyrosine residue located in the N-terminal region? Might GAP activity be regulated by means of a novel intramolecular interaction between the N- and C-termini of BCR, and is it possible that such an interaction is controlled by means of conversions between the phosphorylation and dephosphorylation status (supplementary material Fig. S5)? To test these ideas, we first sought a possible interaction between the N- and C-termini of BCR, using purified recombinant proteins (Fig. 8B). GST-fusion proteins including the BCR N-terminus (GST-BCR-NT) pulled down recombinant proteins containing the BCR C-terminus when tyrosine 177 was changed to phenylalanine (BCR-CT-Y177F), but did not wild-type recombinant BCR (BCR-CT-WT). To confirm these data, the interactions between recombinant BCR proteins, bearing N- or C-termini tagged with either GFP (BCR-NT-GFP) or FLAG (BCR-CT-FLAG), were examined in HEK cells (Fig. 8C). BCR-NT, mimicking dephosphorylation (BCR-NT-Y177F), was co-immunoprecipitated by BCR-CT to an extent much greater than noted when wild-type (BCR-NT-WT) or mutant BCR protein mimicking phosphorylation of tyrosine 177 (BCR-NT-Y177E), was employed. Next, FRET analysis was conducted using constructs with YFP and CFP fused to the N- and C-termini of BCR (YFP-BCR-CFP), and FRET efficiency was examined employing BCR mutants mimicking either dephosphorylation or phosphorylation of tyrosine 177 (Fig. 8D,E). The intensities of FRET signal were enhanced when a mutant mimicking dephosphorylation of tyrosine 177 (Y177F) was employed, in comparison with the wild-type protein or a mutant protein mimicking phosphorylation of tyrosine 177 (Y177E) (Fig. 8F). These results showed that interaction between the N- and C-termini of BCR was enhanced when tyrosine 177 was dephosphorylated via the action of PTPRT. Therefore, the Rac1 GAP activity of BCR could be regulated by means of an intramolecular interaction between N- and C-termini of BCR that is enhanced by dephosphorylation of tyrosine 177.

Fig. 8. GAP activity of BCR is controlled through conversions between the phosphorylation and dephosphorylation of tyrosine residues. (**A**) The GAP activity of BCR was regulated by mutation of tyrosine 177. When BCR-Y177F was co-expressed with the Rac1-FRET sensor in COS-7 cells, the FRET signal was enhanced significantly to a level greater than that seen in the presence of BCR-WT. Note that the FRET signal was not increased by the addition of the epidermal growth factor (EGF, 100 ng/ml) upon co-expression of BCR-WT, whereas it was increased upon single expression of Rac1-FRET sensor (control) or co-expression of BCR-Y177F. Means±s.e.m. of data from thirteen control cells, thirteen BCR-WT cells, and thirteen BCR-Y177F cells are shown. ***$P<0.001$, by the Newman-Keuls multiple comparison test after application of one-way ANOVA; $F=17.10$; $P<0.001$. Scale bar: 10 μm. AU, arbitrary units. (**B**) Interaction between the BCR N- and C-termini was studied using purified GST fusion proteins. The recombinant proteins encoding the BCR C-terminus were pulled down by a GST fusion protein containing the BCR N-terminus, with tyrosine 177 mutated to phenylalanine (BCR-NT-Y177F). However, the wild-type N-terminus (BCR-NT-WT) was ineffective in pulldown. (**C**) Co-immunoprecipitation of the BCR N-terminus by the BCR C-terminus. A recombinant GFP-tagged N-terminal region was co-immunoprecipitated by a BCR C-terminal region tagged with FLAG. The interaction was enhanced by a mutant mimicking dephosphorylation of tyrosine 177 (Y177F) to the level much greater than that with wild-type (WT) protein or a mutant mimicking phosphorylation (Y177E). Quantification (mutated/wild-type BCR): BCR-Y177F, 1.89; BCR-Y177E, 0.64. (**D**) Schematic diagram of the YFP-BCR-CFP construct prepared for the FRET experiment. YFP was tagged to the N-terminus, and CFP to the C-terminus, of BCR. (**E**,**F**) The FRET signal was increased by a mutation mimicking dephosphorylation of tyrosine 177 (Y177F), to an extent greater than noted when wild-type (WT) protein, or a mutation thereof mimicking phosphorylation of tyrosine 177 (Y177E), was employed. The increased FRET signal, indicated by the asterisk, in living COS-7 cells, shows that there is a stronger intramolecular interaction between the N- and C-termini of BCR-Y177F. Five independent FRET tests were performed. Scale bar: 10 μm (E). Means±s.e.m. of data from nine BCR-WT cells, seventeen BCR-Y177F cells and nine BCR-Y177E cells are shown. ***$P<0.001$, by the Newman-Keuls multiple comparison test following application of one-way ANOVA. $F=61.79$; $P<0.0001$ (F). (**G**) The intermolecular interactions of BCR were increased by tyrosine phosphorylation. When two differently tagged BCRs (EGFP or FLAG) were expressed in HEK cells, FLAG-BCR pulled down much more EGFP-BCR via the co-expression of constitutively active Fyn (caFyn) than what was noted in the co-expression of kinase-dead Fyn (kdFyn). 1.5-fold more EGFP-BCR was recruited by FLAG-BCR when co-transfected with caFyn compared with that upon co-transfection with kdFyn. (**H**) The intermolecular interactions of BCR were decreased by dephosphorylation of tyrosine residue. When PTPRT was co-expressed with BCR and Fyn, the multimerization of BCR was decreased by half compared with that without the addition of PTPRT.

The GAP activity of BCR seemed to be regulated by the N-terminal coiled coil (CC) oligomerization domain (Fig. 4A,B). Following this, we examined whether the multimerization of BCR could be controlled by means of conversions between the phosphorylation and dephosphorylation of the tyrosine residue. When full-length BCRs tagged with EGFP or FLAG respectively were expressed in HEK cells, the interaction between differently tagged BCR was significantly increased by co-expression of constitutively active Fyn (caFyn) compared to that by kinase-dead Fyn (kdFyn) (Fig. 8G). Then, PTPRT was additionally expressed in this context of co-expression of BCR and Fyn, and we found that the multimerization of BCR was considerably decreased by the tyrosine dephosphorylation (Fig. 8H). PTPRT appeared to enhance the intramolecular interaction, but to decrease the intermolecular interaction.

BCR GAP activity could be increased when the C-terminal GAP domain was released from N-terminus and the intermolecular interaction of BCR was induced (supplementary material Fig. S5). By contrast, BCR GAP activity was attenuated when the intramolecular interaction was enhanced through the dephosphorylation of tyrosine 177 by PTPRT. Conclusively, BCR and PTPRT together regulate neuronal development via a process involving the Rac1 GTPase signaling pathway controlled by BCR GAP activity that could be attenuated by PTPRT.

Discussion

In the present study, the Rac1 GTPase-activating protein BCR was shown to be a negative regulator of neuronal development. The neuronal tyrosine phosphatase PTPRT inhibited the BCR GAP activity through the tyrosine dephosphorylation of BCR that induced the intramolecular interaction and inhibited the intermolecular interaction of BCR proteins. In the present work, we identified novel functions of BCR and PTPRT that regulate the development of hippocampal neurons.

BCR is a key factor in neuronal development

BCR is known to be a fusion partner of Abl, thus forming BCR-Abl, a characteristic of chronic myelogenous leukemia (Pluk et al., 2002; Ren, 2005). The BCR-Abl fusion protein exhibits the tyrosine kinase activity of Abl, which phosphorylates tyrosine residues of BCR either in the *cis* or in *trans* form. In the present work, we show that Fyn tyrosine kinase and PTPRT tyrosine phosphatase act on tyrosine 177 of BCR for the first time.

Previously, BCR GAP activity was reported to be regulated by direct protein/protein interactions with the Rho guanine nucleotide dissociation inhibitor (Kweon et al., 2008). In the present work, an intramolecular interaction between the N- and C-termini of BCR was enhanced upon dephosphorylation by PTPRT and as a result, we found that BCR GAP activity seemed to be inhibited. On the other hand tyrosine phosphorylation of BCR increased the intermolecular interaction and seemed to enhance the Rac1 GAP activity. Interestingly we show that Rac1 GAP activity of BCR is decreased by deletion of the coiled coil (CC). The N-terminal CC domain of BCR-Abl has been known to control Abl activity by inducing protein multimerization and to promote the association with actin fibers in cancer cells (McWhirter et al., 1993; He et al., 2002; Beissert et al., 2003). Although we cannot exclude the possibility that deletion of the CC negatively affected the assembly of Rac1 and actin fibers, it appeared that both tyrosine phosphorylation and the CC domain could enhance the Rac1 GAP activity through multimerization of BCR.

The expression level of BCR in rat brain decreases from the embryonic stage to early postnatal life, and ABR expression increases until adulthood is attained (Oh et al., 2010). In the early stages of neural circuit development, such processes must be delicately controlled. It seems that Rac1 GAP activity of BCR is regulated by PTPRT. After appropriate neural circuits are formed at the late postnatal stage, ABR seems to become the dominant controller of dendritic arborization, mediated by expression of GAP activity. In hippocampal neurons, BCR GAP activity is controlled via conversions between the intra- and intermolecular interactions that are finely regulated through the dephosphorylation of a specific tyrosine residue by PTPRT. The end result is that BCR Rac1 GAP regulates neuronal development in cooperation with PTPRT.

PTPRT is a key player in the Rac1 signaling pathway

Here, PTPRT was found to control the neuronal development of hippocampal neurons for the first time. When PTPRT was knocked down using a specific shRNA, the dendritc arborization and actin polymerization was inhibited. PTPRT expression may thus be relevant to an understanding of neuronal diseases, including both mental retardation and autism, because PTPRT may control the Rho GTPase signaling pathway by inhibiting the action of the BCR Rac1 GTPase-activating protein. Many genetic diseases associated with neuronal development result from mutations in components of Rho GTPase signaling pathways. Among such conditions, non-syndromic mental retardation may be associated with deletion or mutation of genes located on the X-chromosome (the gene encoding oligophrenin 1; a GAP specific for Rho GTPases, is an example). Other such genes include those encoding PAK3 (p21-activated kinase 3, a serine/threonine kinase functioning downstream of Rac and Cds42) and ARHGEF6 (a GEF specific for Rho GTPases; also known as α-PIX or Cool-2) (Luo, 2000). William's syndrome, a rare neurodevelopmental disorder, is caused by loss of one copy of the LIM kinase gene, the encoded protein of which acts downstream of both Rac and Rho to phosphorylate the actin depolymerization factor cofilin. PTPRT has also been identified as an important component of the Rho GTPase signaling pathway owing to an interaction mediated by BCR Rac1 GAP. PTPRT may thus be a valuable drug target for therapy of neuronal diseases.

In the present work, BCR and PTPRT were shown to regulate neuronal development via the Rac1 GTPase pathway. PTPRT regulates the Rac1 GAP activity of BCR by dephosphorylation of a specific tyrosine residue located in the N-terminal region.

Materials and Methods

DNA constructs

Full-length human BCR (NM_004327, aa 1–1271), human ABR (NM_02162, aa 1–859), and human PTPRT (NM_133170, aa 1–1460) were subcloned into GW1-CMV. BCR-NT and BCR-CT were constructed by subcloning of DNA encoding aa 2–453 and aa 454–1271 of BCR into p3xFLAG-CMV-7.1 (Sigma, St. Louis, MO, USA). BCRΔCC was constructed by deleting aa 27–55 from full-length BCR. To create GAP-dead mutants (BCR-GD and ABR-GD), Arg1090 of BCR and Arg683 of ABR were changed to Ala using the Quick-Change site-directed mutagenesis kit (Agilent Technologies, Santa Clara, CA, USA). For knockdown of rat BCR (XM_228091.4), nt 363–381 (GGTCAACGACAAAGAGGTG, BCR-shRNA) or nt 330–348 (CGTCGAGTTCCACCACGAG, BCR-shRNA*) was subcloned into pSuper.gfp/neo (OligoEngine, Seattle, WA, USA). BCR-shRNAs (Resc BCR and Resc BCR*) were produced by changing underlined nucleotides in the shRNA target region (GGTCAATGATAAAGAGGTG, Resc BCR for BCR-shRNA; CGTCGAATTTCATCACGAG, Resc BCR* for BCR-shRNA*). The Y177F, Y177E, Y283F, Y328F, and Y360F BCR constructs were generated by the Quick-Change site-directed mutagenesis kit. YFP-BCR-CFP was constructed by inserting YFP into the N-terminus of BCR followed by subcloning of YFP-BCR into pECFP-N1 (Clontech, Mountain View, CA, USA). For the construction of

RT-JD, DNA encoding aa 804–1173 of PTPRT was subcloned to into p3xFLAG-CMV-7.1.

Antibodies

Polyclonal antibodies of BCR, ABR, and EGFP were produced as described previously (Oh et al., 2010; Lee et al., 2003). The PTPRT monoclonal antibody was produced in mice as described previously (Lim et al., 2009). The following antibodies were purchased: BCR-N20 (sc-886, Santa Cruz Biotechnology, Santa Cruz, CA, USA), ABR (A80820, BD Biosciences, San Jose, CA, USA), phosphotyrosine (4G10, no. 05-321, Upstate Millipore, Damstadt, Germany), FLAG (M2, F9291, Sigma, Saint Louis, MO, USA), α-tubulin (T8203, Sigma, Saint Louis, MO, USA). Polyclonal antibodies of PSD-95, SSCAM, GRIP, and Homer were described previously (Mok et al., 2002). For immunocytochemistry, hippocampal neurons were incubated with primary antibodies [EGFP (no. 1687; 1:150), BCR (5 mg/ml), ABR (1:60), PTPRT (1:40), FLAG (1:100)] followed by Cy3- or FITC-conjugated secondary antibodies (Jackson ImmunoResearch, West Grove, PA, USA). For western blotting, nitrocellulose membranes were incubated with primary antibodies [BCR (1:1000), EGFP (1:2000), PTPRT (1:2000), phosphotyrosine (1:1000), FLAG (1:1000), α-tubulin (1:2000)].

Transfection of neurons, immunocytochemistry, and F-actin staining

Primary hippocampal neurons were prepared from embryonic day 18 (E18) rats, grown on glass coverslip, and transfected using the calcium phosphate method at 5 or 7 d *in vitro* (DIV), as described previously (Lim et al., 2009). At 9~10 DIV, hippocampal neurons were fixed in 4% (v/v) formaldehyde/4% (w/v) sucrose, permeabilized with 0.2% (v/v) Triton X-100 in phosphate-buffered saline, incubated with primary antibodies, and finally incubated with fluorophore-conjugated secondary antibodies (Jackson ImmunoResearch Laboratories, West Glove, PA, USA). To visualize polymerized actin (F-actin) in hippocampal neurons, phalloidin conjugated with Alexa Fluor 555 (Life Technologies, Grand Island, NY, USA), diluted 1:20, was mixed with secondary antibody solutions for 2 h.

Image analysis and quantification

Sholl analysis was performed employing the modified method of Nakayama et al. (Nakayama et al., 2000). Individual neurons were imaged using a 20×objective, employing confocal microscopy (LSM 510 Meta, Zeiss, Gottingen, Germany), and images were printed. To obtain the Sholl profiles of dendritic arbors, printouts were placed under a clear sheet featuring concentric circles with diameters increasing in 20 μm increments. The center of the circles was placed at the cell body center and the numbers of dendrites crossing each concentric circle were counted. Quantification of primary and secondary dendrites was also performed by imaging of individual neurons using a 20× objective. For quantification of F-actin fluorescence intensity, images of each hippocampal neuron stained by Alexa Fluor 555-phalloidin were acquired using a 40× objective. The average pixel intensities on all dendritic trunks of hippocampal neurons were measured 20 μm distant from the neuronal soma using the MetaMorph software (Molecular Devices, Sunnyvale, CA, USA). For the negative control of F-actin staining, hippocampal neurons were treated by Latrunculin A, an inhibitor of actin polymerization, for 12 hrs. All analyses and quantification were performed blind.

Rat brain synaptosome preparation

Rat whole brain was removed, dissected into ice-cold into 10 volumes of cold homogenization buffer (0.32 M sucrose, 4 mM HEPES-NaOH, 1 mM $MgCl_2$, 0.5 mM $CaCl_2$, pH 7.3 with inhibitors of protease and phosphatase), and homogenized using glass homogenizer. Whole homogenate of rat brain was spun at 1000 ***g*** for 15 min to remove nuclear fraction. The resulting supernatant was spun at 12,000 ***g*** for 15 min to yield pelleted crude synaptosome. Crude synaptosome was resuspended in suitable volume (1 ml/g of tissue) of ice-cold Tris-EDTA buffer (10 mM Tris-HCl, 5 mM EDTA, pH 7.4), added with 1% sodium deoxycholate, and then incubated in 37℃ for 30 min. The solubilized synaptosome was added with 0.1% Triton X-100 and subjected to dialysis against cold 0.1% Triton X-100 in 50 mM Tris-HCl buffer, pH 7.4.

Co-immunoprecipitation studies

Sodium deoxycholate extracts of the rat synaptosome were incubated with an anti-PTPRT monoclonal antibody (Lim et al., 2009) or non-immune mouse immunoglobulin (IgG), and co-immunoprecipitated BCR was probed using an anti-BCR antibody (Santa Cruz Biotechnology, Santa Cruz, CA, USA; catalog no. sc-886). BCR and PTPRT were expressed in HEK293 cells and cleared lysates of such cells were incubated with anti-BCR or anti-PTPRT antibodies. Co-immunoprecipitated PTPRT and BCR were loaded onto SDS-PAGE gels and subjected to western blotting using appropriate antibodies.

FRET

Rac1 FRET-sensor construct which induces a FRET signal by activation of Rac1 GTPase (Itoh et al., 2002; Itoh et al., 2008) was transfected into COS-7 cells with BCR-WT or BCR-mutant mimicking dephosphorylation of tyrosine 177 (Y177F) respectively. After 48 hr, the FRET images from living cells were captured using FRET software pre-equipped on confocal microscopy (LSM 510 Meta, Zeiss). CFP and YFP were excited with the 405 and 514 nm line of an argon laser respectively. Emitted fluorescence was collected at 420–480 nm for CFP and 530–600 nm for YFP. After adding of the epidermal growth factor (EGF, 100 ng/ml) to the culture media, the FRET images of Rac1 FRET sensor-expressed cells were captured every 3 min. The FRET images were transferred onto the MetaMorph software (Molecular Devices) and the intensities of the FRET signal were analyzed at more than three regions of the transfected cells.

The YFP-BCR-CFP constructs were transfected into COS-7 cells in order to induce a FRET signal when the interactions between the N- and C-termini of BCR were enhanced. YFP and CFP were fused into N- or C-termini of wild type BCR, BCR mutant mimicking dephosphorylation of tyrosine 177 (Y177F), and BCR mutnant mimicking phosphorylation of tyrosine 177 (Y177E) respectively. After 48 hr, the FRET images from living cells were captured using the FRET software pre-equipped on the LSM 510 Meta confocal microscope (Zeiss) and transferred onto the MetaMorph software for analysis. The intensity of the FRET signal were measured and analyzed at more than three region of the transfected cells with the MetaMorph software.

In vitro tyrosine phosphatase assay

BCR was expressed in HEK293 cells treated with 200 mM pervanadate for 15 min, 2 days after transfection. Cleared lysates of cells solubilized in 1% (v/v) Triton X-100 in PBS were incubated with an anti-BCR antibody bound to protein A-agarose and next washed four times. Immunoprecipitated BCR was incubated with purified recombinant protein containing the PTPRT catalytic domain, for 30 min at 25℃ (Lim et al., 2009). Reactions were terminated by addition of SDS sample buffer, and the tyrosine phosphorylation status of BCR was probed using an anti-phosphotyrosine antibody (Millipore, Billerica, MA, USA).

Statistics

Results are expressed as means±s.e.m. and one-way ANOVA followed by application of the Newman-Keuls multiple comparison test was used to assess statistical significance. A comparison was considered to be significant if $P<0.05$.

Acknowledgements

We would like to thank Dr Owen Witte (UCLA, USA) for human BCR cDNA, Dr Louis Lim (University College London, UK) for human ABR cDNA, and Dr Michiyuki Matsuda (Kyoto University, Japan) for the Rac1-FRET sensor.

Funding

This research was supported by the Basic Science Research Program through the National Research Foundation of Korea (NRF) grant funded by the Korea government (MEST) [grant number 2011-0027399 to J.R.L.]; a grant from Korea Research Institute of Bioscience and Biotechnology research initiative program (to J.R.L.); and the joint research collaboration program for Chinese-Korean-Japanese research co-operation (to D.Y.Y.).

Supplementary material available online at
http://jcs.biologists.org/lookup/suppl/doi:10.1242/jcs.105502/-/DC1

References

Beissert, T., Puccetti, E., Bianchini, A., Güller, S., Boehrer, S., Hoelzer, D., Ottmann, O. G., Nervi, C. and Ruthardt, M. (2003). Targeting of the N-terminal coiled coil oligomerization interface of BCR interferes with the transformation potential of BCR-ABL and increases sensitivity to STI571. *Blood* **102**, 2985-2993.

Bosco, E. E., Mulloy, J. C. and Zheng, Y. (2009). Rac1 GTPase: a "Rac" of all trades. *Cell. Mol. Life Sci.* **66**, 370-374.

Carlisle, H. J. and Kennedy, M. B. (2005). Spine architecture and synaptic plasticity. *Trends Neurosci.* **28**, 182-187.

Chen, H. and Firestein, B. L. (2007). RhoA regulates dendritic branching in hippocampal neurons by decreasing cypin protein levels. *J. Neurosci.* **27**, 8378-8386.

Chen, Q., Zhu, Y. C., Yu, J., Miao, S., Zheng, J., Xu, L., Zhou, Y., Li, D., Zhang, C., Tao, J. et al. (2010). CDKL5, a protein associated with rett syndrome, regulates neuronal morphogenesis via Rac1 signaling. *J. Neurosci.* **30**, 12777-12786.

Chiu, S. L., Chen, C. M. and Cline, H. T. (2008). Insulin receptor signaling regulates synapse number, dendritic plasticity, and circuit function in vivo. *Neuron* **58**, 708-719.

Chuang, T. H., Xu, X., Kaartinen, V., Heisterkamp, N., Groffen, J. and Bokoch, G. M. (1995). Abr and Bcr are multifunctional regulators of the Rho GTP-binding protein family. *Proc. Natl. Acad. Sci. USA* **92**, 10282-10286.

Diekmann, D., Brill, S., Garrett, M. D., Totty, N., Hsuan, J., Monfries, C., Hall, C., Lim, L. and Hall, A. (1991). Bcr encodes a GTPase-activating protein for p21rac. *Nature* **351**, 400-402.

Giubellino, A., Burke, T. R., Jr and Bottaro, D. P. (2008). Grb2 signaling in cell motility and cancer. *Expert Opin. Ther. Targets* **12**, 1021-1033.

He, Y., Wertheim, J. A., Xu, L., Miller, J. P., Karnell, F. G., Choi, J. K., Ren, R. and Pear, W. S. (2002). The coiled-coil domain and Tyr177 of bcr are required to induce a murine chronic myelogenous leukemia-like disease by bcr/abl. *Blood* **99**, 2957-2968.

Heisterkamp, N., Morris, C. and Groffen, J. (1989). ABR, an active BCR-related gene. *Nucleic Acids Res.* **17**, 8821-8831.

Itoh, R. E., Kurokawa, K., Ohba, Y., Yoshizaki, H., Mochizuki, N. and Matsuda, M. (2002). Activation of rac and cdc42 video imaged by fluorescent resonance energy transfer-based single-molecule probes in the membrane of living cells. *Mol. Cell Biol.* **22**, 6582-6591.

Itoh, R. E., Kiyokawa, E., Aoki, K., Nishioka, T., Akiyama, T. and Matsuda, M. (2008). Phosphorylation and activation of the Rac1 and Cdc42 GEF Asef in A431 cells stimulated by EGF. *J. Cell Sci.* **121**, 2635-2642.

Kawashima, T., Hirose, K., Satoh, T., Kaneko, A., Ikeda, Y., Kaziro, Y., Nosaka, T. and Kitamura, T. (2000). MgcRacGAP is involved in the control of growth and differentiation of hematopoietic cells. *Blood* **96**, 2116-2124.

Kweon, S. M., Cho, Y. J., Minoo, P., Groffen, J. and Heisterkamp, N. (2008). Activity of the Bcr GTPase-activating domain is regulated through direct protein/protein interaction with the Rho guanine nucleotide dissociation inhibitor. *J. Biol. Chem.* **283**, 3023-3030.

Lee, J. R., Shin, H., Ko, J., Choi, J., Lee, H. and Kim, E. (2003). Characterization of the movement of the kinesin motor KIF1A in living cultured neurons. *J. Biol. Chem.* **278**, 2624-2629.

Li, J. and Smithgall, T. E. (1996). Co-expression with BCR induces activation of the FES tyrosine kinase and phosphorylation of specific N-terminal BCR tyrosine residues. *J. Biol. Chem.* **271**, 32930-32936.

Li, S., Couvillon, A. D., Brasher, B. B. and Van Etten, R. A. (2001). Tyrosine phosphorylation of Grb2 by Bcr/Abl and epidermal growth factor receptor: a novel regulatory mechanism for tyrosine kinase signaling. *EMBO J.* **20**, 6793-6804.

Lim, S. H., Kwon, S. K., Lee, M. K., Moon, J., Jeong, D. G., Park, E., Kim, S. J., Park, B. C., Lee, S. C., Ryu, S. E. et al. (2009). Synapse formation regulated by protein tyrosine phosphatase receptor T through interaction with cell adhesion molecules and Fyn. *EMBO J.* **28**, 3564-3578.

Liu, J., Wu, Y., Ma, G. Z., Lu, D., Haataja, L., Heisterkamp, N., Groffen, J. and Arlinghaus, R. B. (1996). Inhibition of Bcr serine kinase by tyrosine phosphorylation. *Mol. Cell Biol.* **16**, 998-1005.

Luo, L. (2000). Rho GTPases in neuronal morphogenesis. *Nat. Rev. Neurosci.* **1**, 173-180.

Maru, Y., Peters, K. L., Afar, D. E., Shibuya, M., Witte, O. N. and Smithgall, T. E. (1995). Tyrosine phosphorylation of BCR by FPS/FES protein-tyrosine kinases induces association of BCR with GRB-2/SOS. *Mol. Cell Biol.* **15**, 835-842.

McWhirter, J. R., Galasso, D. L. and Wang, J. Y. (1993). A coiled-coil oligomerization domain of Bcr is essential for the transforming function of Bcr-Abl oncoproteins. *Mol. Cell Biol.* **13**, 7587-7595.

Mok, H., Shin, H., Kim, S., Lee, J. R., Yoon, J. and Kim, E. (2002). Association of the kinesin superfamily motor protein KIF1Ba with PSD-95, SAP-97, and SSCAM. *J. Neurosci.* **22**, 5253-5258.

Nakayama, A. Y., Harms, M. B. and Luo, L. (2000). Small GTPases Rac and Rho in the maintenance of dendritic spines and branches in hippocampal pyramidal neurons. *J. Neurosci.* **20**, 5329-5338.

Neubrand, V. E., Thomas, C., Schmidt, S., Debant, A. and Schiavo, G. (2010). Kidins220/ARMS regulates Rac1-dependent neurite outgrowth by direct interaction with the RhoGEF Trio. *J. Cell Sci.* **123**, 2111-2123.

Oh, D., Han, S., Seo, J., Lee, J. R., Choi, J., Groffen, J., Kim, K., Cho, Y., Choi, H. S., Shin, H. et al. (2010). Regulation of synaptic Rac1 activity, long-term potentiation maintenance, and learning and memory by BCR and ABR Rac GTPase-activating proteins. *J. Neurosci.* **30**, 14134-14144.

Peng, Y. R., He, S., Marie, H., Zeng, S. Y., Ma, J., Tan, Z. J., Lee, S. Y., Malenka, R. C. and Yu, X. (2009). Coordinated changes in dendritic arborization and synaptic strength during neural circuit development. *Neuron* **61**, 71-84.

Pluk, H., Dorey, K. and Superti-Furga, G. (2002). Autoinhibition of c-Abl. *Cell* **108**, 247-259.

Ren, R. (2005). Mechanisms of BCR-ABL in the pathogenesis of chronic myelogenous leukaemia. *Nat. Rev. Cancer* **5**, 172-183.

Ress, A. and Moelling, K. (2005). Bcr is a negative regulator of the Wnt signalling pathway. *EMBO Rep.* **6**, 1095-1100.

Rosso, S. B., Sussman, D., Wynshaw-Boris, A. and Salinas, P. C. (2005). Wnt signaling through Dishevelled, Rac and JNK regulates dendritic development. *Nat. Neurosci.* **8**, 34-42.

Scott, E. K. and Luo, L. (2001). How do dendrites take their shape? *Nat. Neurosci.* **4**, 359-365.

Sfakianos, M. K., Eisman, A., Gourley, S. L., Bradley, W. D., Scheetz, A. J., Settleman, J., Taylor, J. R., Greer, C. A., Williamson, A. and Koleske, A. J. (2007). Inhibition of Rho via Arg and p190RhoGAP in the postnatal mouse hippocampus regulates dendritic spine maturation, synapse and dendrite stability, and behavior. *J. Neurosci.* **27**, 10982-10992.

Sini, P., Cannas, A., Koleske, A. J., Di Fiore, P. P. and Scita, G. (2004). Abl-dependent tyrosine phosphorylation of Sos-1 mediates growth-factor-induced Rac activation. *Nat. Cell Biol.* **6**, 268-274.

Tahirovic, S., Hellal, F., Neukirchen, D., Hindges, R., Garvalov, B. K., Flynn, K. C., Stradal, T. E., Chrostek-Grashoff, A., Brakebusch, C. and Bradke, F. (2010). Rac1 regulates neuronal polarization through the WAVE complex. *J. Neurosci.* **30**, 6930-6943.

Tan, E. C., Leung, T., Manser, E. and Lim, L. (1993). The human active breakpoint cluster region-related gene encodes a brain protein with homology to guanine nucleotide exchange proteins and GTPase-activating proteins. *J. Biol. Chem.* **268**, 27291-27298.

Tauchi, T., Miyazawa, K., Feng, G. S., Broxmeyer, H. E. and Toyama, K. (1997). A coiled-coil tetramerization domain of BCR-ABL is essential for the interactions of SH2-containing signal transduction molecules. *J. Biol. Chem.* **272**, 1389-1394.

Van Aelst, L. and Cline, H. T. (2004). Rho GTPases and activity-dependent dendrite development. *Curr. Opin. Neurobiol.* **14**, 297-304.

Voncken, J. W., van Schaick, H., Kaartinen, V., Deemer, K., Coates, T., Landing, B., Pattengale, P., Dorseuil, O., Bokoch, G. M., Groffen, J. et al. (1995). Increased neutrophil respiratory burst in bcr-null mutants. *Cell* **80**, 719-728.

Zhang, X., Subrahmanyam, R., Wong, R., Gross, A. W. and Ren, R. (2001). The NH_2-terminal coiled-coil domain and tyrosine 177 play important roles in induction of a myeloproliferative disease in mice by Bcr-Abl. *Mol. Cell Biol.* **21**, 840-853.

Zhao, Y., Zhang, X., Guda, K., Lawrence, E., Sun, Q., Watanabe, T., Iwakura, Y., Asano, M., Wei, L., Yang, Z. et al. (2010). Identification and functional characterization of paxillin as a target of protein tyrosine phosphatase receptor T. Proc. *Natl. Acad. Sci. USA* **107**, 2592-2597.